Int. J. Electrochem. Sci., 14 **(2019)** 5508 – 5520, doi: 10.20964/2019.06.39

International Journal of
ELECTROCHEMICAL
SCIENCE
www.electrochemsci.org

Sulfonation of Poly(phenylene oxide) Anion Exchange Membrane for All Vanadium Flow Redox Battery

Nanfang Wang[1,*], *Fan Zhang*[1], *Ru Zhang*[1], *Wenchang Zhou*[1], *Dan Lu*[2]

[1] Hunan Provincial Key Laboratory of Environmental Catalysis & Waste Recycling, School of Chemistry and Chemical Engineering, Hunan Institute of Engineering, Xiangtan 411104, China
[2] Hunan Corun New Energy Co., Ltd., Changsha 410205, China
[*]E-mail: cdwnf@126.com

Received: 4 February 2019 / *Accepted:* 28 March 2019 / *Published:* 10 May 2019

To develop a low cost non-fluorinated membrane for vanadium redox flow battery (VRFB), several commercial ion exchange membranes (IEM) were compared in terms of primary properties such as ion exchange capacity (*IEC*), vanadium ion permeability (*P*) and water transfer (*WT*) and chemical stability, and an anion exchange membrane (AEM) DF-a (based on Poly(phenylene oxide) polymers) was sulfonated into amphoteric ion exchange membranes (DF-a1 and DF-a2) to restrain *WT*. Effects of sulfonation on morphologies, selective proton conductivity (σ), *WT* and chemical stability of membranes were investigated. The results showed that sulfonation can improve *IEC, σ, Selectivity* and chemical stability of the AEM (DF-a). Due to Donnan effect, DF-a2 had a more dramatic reduction in *WT* and self discharge in VRFB than DF-a. Cell test showed that the membrane DF-a2 had higher coulombic efficiency (*CE*) and energy efficiency (*EE*) than DF-a and DF-a1, possessing a better potential application in VRFB.

Keywords: Amphoteric membrane; Sulfonation; Vanadium permeability; Water transfer; Vanadium redox flow battery

1. INTRODUCTION

Clean energy is indispensable for human society sustainable development. A clean and renewable energy source like solar or wind power will be an alternative to fossil fuels. Electrical energy storage (EES) is an effective means to smooth the intermittency of renewable energy production and maintain the continuousness and stability of its electricity supplies. All vanadium redox flow battery (VRFB) is regarded as a promising large-scale power conservation system due to its outstanding properties such as long cycle life, flexible design, fast response time, deep-discharge capacity, and low cost in energy storage [1-4]. VRFB employs VO^{2+}/VO_2^{+} and V^{2+}/V^{3+} redox couples in the positive and negative half-cell electrolytes, respectively, which are separated by an ion exchange

membrane (IEM). The role of IEM is to prevent cross mixing of the positive and negative electrolytes, while allowing the transport of ions such as proton to complete the current circuit during the charge/discharge state. Ideally, IEM should possess such properties as high proton conductivity, low vanadium ion permeability, good chemical stability, and low price [5, 6]. Perfluorosulfonic polymer membranes like Du Pont Nafion® are currently used as a separator in VRFB [5, 7] due to their excellent proton conductivity for a high voltage efficiency (*VE*) and chemical stability for a long cycle life. However, the large-scale application is curbed mainly by their high cost and other shortcomings including great vanadium ion permeability [6] and severe water transfer [8] which can lead to the decrease in coulombic efficiency (*CE*) and energy efficiency (*EE*). These limitations have triggered many efforts in developing alternative membranes [9]. So far, sulfonated aromatic polymer membranes including SPEEK, SPES, and SPESK have been developed for VRFB due to their low price, good ionic conductivity, and excellent mechanical properties [10-18]. But there is a long and painful way to apply them in VRFB practically.

The low cost and non-fluorinated IEMs with desired ionic exchange capacity (*IEC*), good resistance to acid, alkali and most oxidants are conventionally applied in chemical separation such as metallurgy, water treatment, food industry, and chlor-alkali industry. There are many reports about assessment and modification [19-22]. However, they are mostly based on Polyethylene (PE) main chain which is not resistant to strong oxidation of V(V) solution.

In this paper, several conventional IEMs were studied in terms of *IEC*, area resistance, vanadium permeability, chemical stability to evaluate the feasibility for VRFB, then an anion IEM (DF-a) containing poly(phenylene oxide) was chosen for sulfonation modification using two methods. The surface and cross-section of the membranes were analyzed by a scanning electron microscope technique (SEM-EDS). The influence of sulfonating modification on primary and electrochemical properties of the membrane was investigated. Performances of VRFB single cell with the modified membranes were evaluated in terms of open circuit voltage (*OCV*), charge-discharge curves, *CE*, *VE*, and *EE*, compared with the pristine DF-a.

2. EXPERIMENTAL

2.1 Materials

Several membrane samples are listed in Table 1. Concentrated sulfuric acid (98 wt.%), potassium dichromate, and other chemical agents were commercially available. 5% perfluorinated sulfonic acid 2-propanol solution (PFSA, D-520) was purchased from DuPont Co., USA. All water utilized was deionized, and all chemicals were used as received without further purification.

Table 1. Commercial membrane samples.

Membrane	Type	Appearance	Thickness (μm)
Nafion117	MCEM	Transparent	130
utx-c	MCEM	Transparent brown	110

utx-a	MAEM	Transparent yellow	120
DF-c	MCEM	Transparent brown	270
DF-a	MAEM	Transparent yellow	310
3369	TCEM	Opaque brown	420
3368	TAEM	Opaque green	420

Note: MCEM is homogeneous cation exchange membrane, MAEM is homogeneous anion exchange membrane, TCEM is heterogeneous cation exchange membrane, TAEM is heterogeneous anion exchange membrane.

2.2 Sulfonating modification of DF-a membrane

DF-a is an anion membrane of poly(phenylene oxide)s which have good mechanical properties, thermal and chemical stability for high-performance engineering plastics due to the backbones containing rigid and thermally stable phenyl moieties and flexible and heat resistant oxygen ether bonds. To incorporate -SO_3H groups into the DF-a membrane, two type sulfonating methods were employed. For type I, a dried DF-a membrane (15 cm×18 cm) was sulfonated using 98 wt.% concentrated sulfuric in addition of 2 wt.% potassium dichromate as a catalyst at room temperature for 0.5 h. After sulfonation, the membrane was rinsed by deionized water to remove the remaining sulfuric acid and then kept in deionized water (denoted as DF-a1). For type II, a dried DF-a membrane sample (5 cm×18 cm) was soaked in a 2 wt.% PFSA 2-propanol solution at room temperature for 12 h. The membrane was dried at 100 ºC for 4 h and then kept in deionized water (denoted as DF-a2). Both the morphologies and energy dispersive X-ray spectroscopy (EDS) of the membranes were observed by a JSM-6360LV Scanning Electron Microscope.

2.3 Membrane properties

The modified membranes are amphoteric exchange membranes so that they contain the anionic ion exchange capacity (IEC_A) [23] and the cationic ion exchange ion exchange (IEC_C) [24], respectively. The *IEC of* the membranes was calculated by the following equation.

$$IEC = IEC_A + IEC_C \quad (1)$$

Water uptake was calculated according to the following equation [25]:

$$\text{Water uptake } (\%) = \frac{W_w - W_d}{W_d} \times 100\% \quad (2)$$

where W_w and W_d are the weight of the wet and dry membrane, respectively.

The area resistance (*AR*) of membranes was tested according to the method in Ref. [26]. Before testing, the membrane sample was soaked in a 1.5 M $VOSO_4$ + 3.0 M H_2SO_4 solution for 24 h. A testing cell was separated by the membrane sample into two compartments filled with 1.5 M $VOSO_4$ + 3.0 M H_2SO_4 solution respectively. Two platinum electrodes (1 cm×1 cm) were held at a fixed distance apart and with a constant immersion depth. The effective area of membrane (*S*) was 1.0 cm^2. The electrochemical impedance spectroscopies (EIS) of the cell with membrane (r_1) and without membrane (r_2) were measured by using a PARAST electrochemistry workstation (USA, AMETEK,

Inc.) over a frequency range of 100 kHz to 100 mHz at room temperature. So, r_1 and r_2 were obtained by interpolating the impedance data to the real axis on the high frequency side (49535~39194Hz), respectively. *AR* (Ωcm^2) was calculated as follows.

$$AR = (r_1 - r_2)S \quad (3)$$

The membrane proton conductivity (σ) was calculated as follows [27].

$$\sigma = \frac{d}{AR} \quad (4)$$

where *d* and *AR* were the membrane thickness and area resistance, respectively.

Permeability of vanadium ions through the membrane sample was investigated using the equipment as in Ref. [28]. As shown in Fig. 1, the left reservoir was filled with a vanadium ion solution of 1.5 M $VOSO_4$ in 3.0 M H_2SO_4 and the right one was filled with a 1.5 M $MgSO_4$ in 3.0 M H_2SO_4 solution, respectively. $MgSO_4$ was used for balancing the ionic strength and eliminating the osmotic pressure. The membrane area (*A*) exposed to the solution was 3 cm×3 cm and the solution volume of both sides was 30 mL. The two solutions were continuously stirred during testing at room temperature. At a regular time interval, solution samples from the right reservoir were taken for determining the vanadium ions concentration by a UV–vis spectrometer (TU-1901). The vanadium ion permeability (*P*) is obtained as the following equation [29, 30].

$$V_R \frac{dc_R(t)}{dt} = A\frac{P}{L}[c_L - c_R(t)] \quad (5)$$

where c_L is the initial vanadium ion concentration in the left reservoir, and $c_R(t)$ is the vanadium ion concentration in the right reservoir with time. *A* and *L* refer to the exposed area and thickness of the membrane, respectively. *P* is the vanadium ion permeability, and V_R is the right reservoir volume. It is supposed that the change of vanadium ion concentration in the left reservoir can be unchanged and a pseudo-steady-state condition can be used inside the membrane.

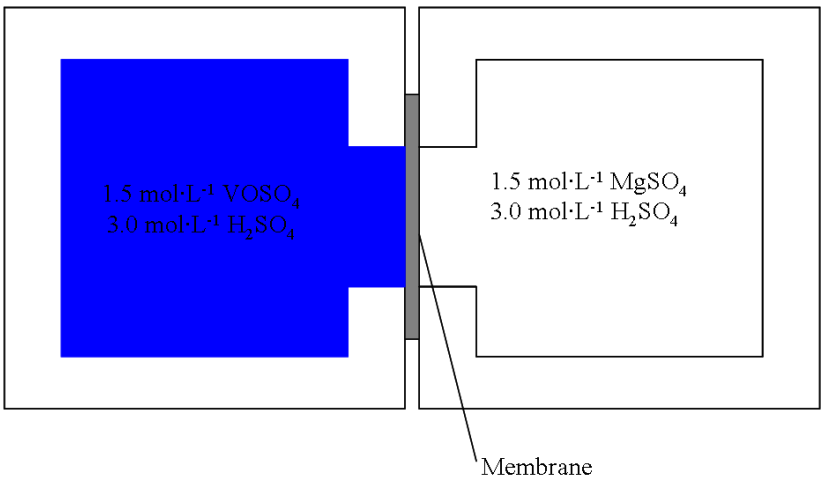

Figure 1. Equipment for the measurement of permeability of VO^{2+}.

Water transfer was determined on a dynamic cell (in VRFB single cell tests Section) at room temperature. In Fig. 2, 120 mL 1.5 mol/L positive and negative vanadium electrolyte solutions with 50% state of charge (SOC) were placed in negative and positive tanks and circulated by pumps

through the negative and positive electrode separated by the membrane sample. The solution heights in both tanks were recorded by reading rulers at intervals.

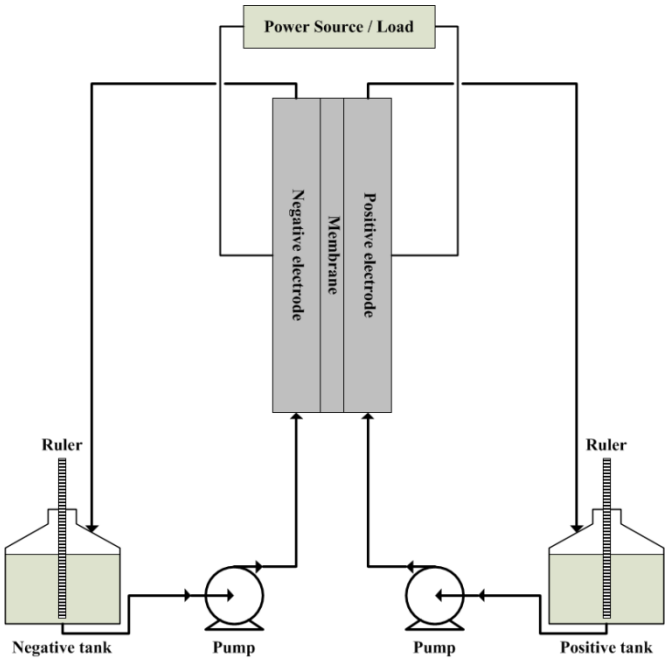

Figure 2. Scheme for water transfer measurement of membrane.

The chemical stability of the membranes was evaluated by immersion in V(V) solution similar to the previously reported method [11]. Membrane samples of size 25 mm × 25 mm and electrolyte solutions (25 mL 1.0 M VO_2^+ / 3 M H_2SO_4) were placed in sealed glass bottles and held without agitation at room temperature. During the immersion tests, 1 mL aliquots from the test bottles were removed at a regular time interval, and the concentration of V(IV) ion was measured by a UV-Vis spectroscopy (TU-1901). After immersion for 30d, weight losses of membrane samples were determined.

2.4 VRFB single cell tests

The tested cell was fabricated by sandwiching the membrane between two pieces of carbon felt electrodes (5 cm thickness, Shenhe carbon fiber Materials Co., Ltd.) with the effective area of 5×6 cm^2, and conductive plastic current collectors (Luhua plastic factory, China). 120 mL negative and positive electrolyte solutions containing 1.5 M V(III)/V(IV) (mol/mol=1:1) complex vanadium sulfate in 3.0 M H_2SO_4 were cyclically pumped respectively through the corresponding half cell by two magnetic pumps (MP-10RN, Shanghai Xinxishan Industrial Co., Ltd., China) with a flow rate of 500 mL/min. The single cell was charged and discharged by a CT2001C-10V/2A battery test system (Wuhan Land Co., Ltd.) at room temperature. To avoid the corrosion of the carbon felt electrodes and conductive plastic, the upper limit of charge voltage was 1.7 V and the lower limit of discharge voltage was 0.7 V.

3. RESULTS AND DISCUSSION

3.1 Comparative study of the common commercial membranes

3.1.1 Primary properties

Table 1 lists the primary properties of studied commercial membranes. The homogeneous ion exchange membranes are transparent while the heterogeneous ion exchange membranes are opaque, which is attributed to their different microstructures. In the fabrication of homogeneous ion exchange membranes, there are no phase separations in the aggregation structures or the micro-phase separation sizes are less than 400~700 nm (visible light wavelength), which results in transparency to visible light. On the contrary, there are more large-size micro-phase separations in the heterogeneous ion exchange membranes so that they are less transparent to visible light [31]. Table 2 presents the primary properties of several commercial membranes including water uptake, *IEC*, *AR*, *P*, and water transfer. It is seen that, regardless of the membrane type, water uptake of the membranes is increased with *IEC*, due to the fact that the ion exchange groups are hydrophilic. The more hydrophilic groups carried in the given membrane region, the more water molecule absorbed [32]. In Table 2, Nafion 117 has the most *P* and water transfer due to its lager pronounced hydrophobic/hydrophilic separation regions [33] than the other non-fluorinated IEMs.

Table 2. Primary properties of commercial membranes.

Membrane	Water uptake (%)	*IEC* (mmol/g)	*AR* (Ωcm^2)	*P* ($\times 10^{-7}$ cm/min)	Water transfer ($\times 10^{-3}$ cm/min)
Nafion117	19.3	0.94	0.94	227.78	29.46
utx-c	21.7	1.22	5.37	42.92	8.750
utx-a	19.4	1.03	7.13	17.22	29.13
DF-c	48.2	1.25	2.88	21.32	14.00
DF-a	52.1	1.40	2.37	35.52	23.38
3369	51.6	1.46	29.06	17.36	1.567
3368	45.6	1.38	46.63	0.0	0.0

3.1.2 Chemical stability in V(V) solution

In VRFB, the positive electrolyte has strong acid and oxidation from V(V) ion, especially in high SOC, so that the membrane as VRFB separator is required to resist to the oxidation degradation [11]. Fig. 3 shows the relationship between V(IV) ion concentration and time. For Nafion 117, V(IV) concentration is almost 0 mol/L during 30 d. For DF-a and utx-a, the curves are upper similar to that of Nafion 117. For DF-c, the V(IV) ion concentration change is much great than the other membranes. Table 3 indicates the weight loss and reduction percentage of V(V) ion for membrane samples in1.0 M V(V) solution after 30 d. Weight losses and reduction percentages of V(V) ion decreased in the order: DF-c > utx-a > DF-a >> Nafion117. The results indicate DF-a has a good chemical stability in V(V) solution for application in VRFB.

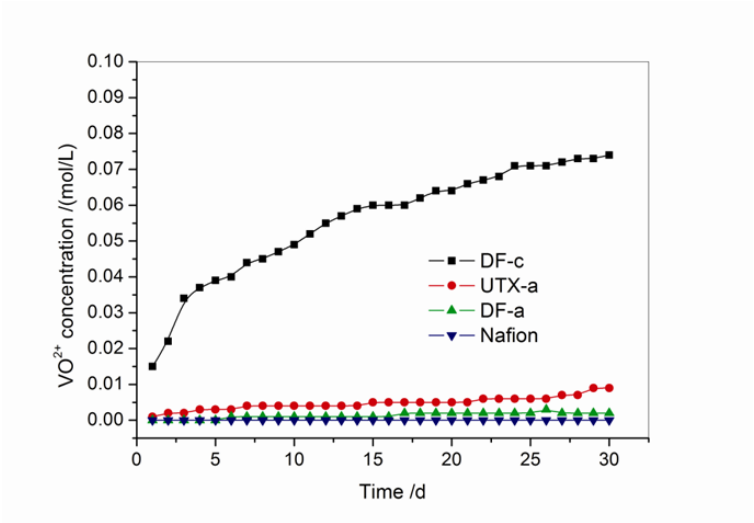

Figure 3. V(IV) concentration vs. time for Nafion117, DF-c, DF-a and utx-a membranes.

Table 3. Chemical stability of membranes in 1.0 M V(V) solution for 30 d.

Membrane	Weight loss/%	Reduction of VO_2^+(%)
Nafion117	0	0.17
DF-a	22.71	3.0
DF-c	51.77	74.60
utx-a	31.68	10.00

3.2 Effect of sulfonation on membrane morphologies

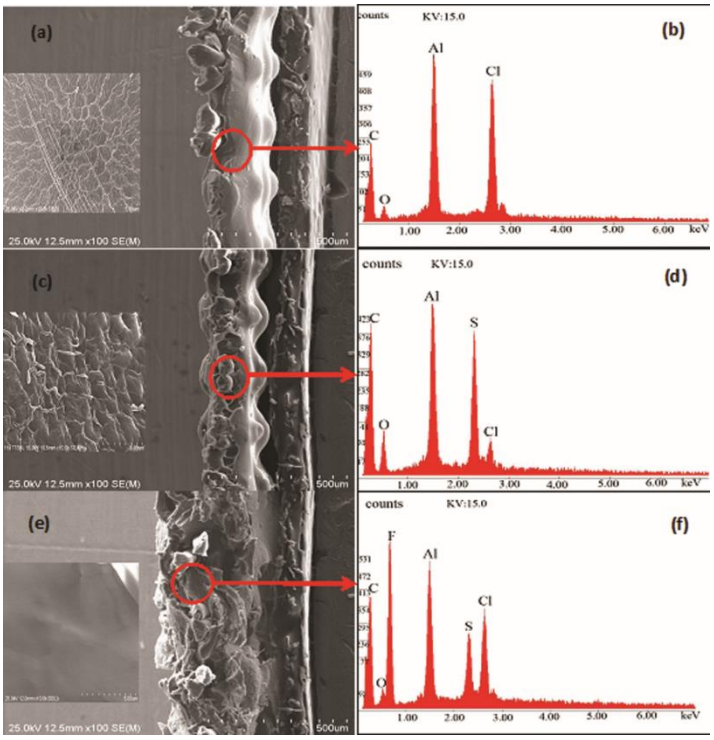

Figure 4. SEM-EDS of membranes. (a) and (b): DF-a; (c) and (d): DF-a1; (e) and (f): DF-a2.

Fig. 4 shows SEM-EDS of the membranes before and after sulfonation. The membrane DF-a1 (Fig. 4c) became thinner than DF-a (Fig. 4a) due to the acidity and oxidation of the concentrated sulfuric acid. The S element in EDS spectra of Fig. 3b and Fig. 3d indicates that -SO_3H groups are successfully introduced. There are some decreases in the strength of Al and Cl peaks probably ascribed to dissolution of some Al_2O_3 and degradation of some polymer binder with Cl element. By comparing Fig. 4a and Fig. 4e, the membrane DF-a2 became thicker and denser in the surface due to the formation of interpenetrating polymer networks in the hydrophilic pores of the base membrane (DF-a). Fig. 4f shows that S peak indicates the introduction of -SO_3H groups on the modified membrane and that the Al and Cl peaks are weaken than that of DF-a indicating the formation of interpenetrating polymer networks.

3.3 Effect of sulfonation on IEC and selectivity

Table 4. Comparison of properties for the membrane samples.

Membranes	Thickness (μm)	*IEC* (mmol/g)	σ (S m^{-1})	*P* ($10^{-7}cm^2/min$)	*Selectivity* [a] (10^4 $minS/cm^3$)
DF-a	310	1.40	1.31	35.52	0.369
DF-a1	303	1.85	1.35	36.00	0.375
DF-a2	350	1.90	1.40	30.34	0.461

a $Selectivity = \frac{\sigma}{P}$

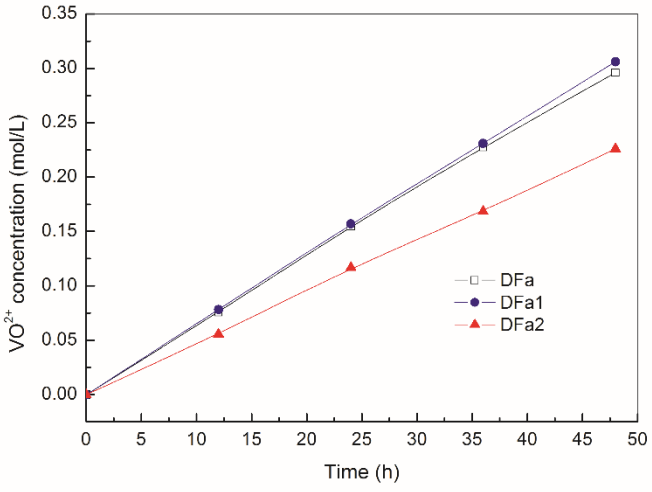

Figure 5. Relation between V(IV) concentration and time in the right reservoir.

Table 4 lists *IEC*, σ, *P* and *Selectivity* of the membranes. *IEC* and σ of the DF-a1 and DF-a2 membranes are higher than that of the DF-a due to introducing -SO_3H groups to DF-a membrane. Water and ions move through the interconnected hydrated ionic channel structure of IEM [33]. The size and morphological details of the ionic domains play an important role in proton conductivity and

vanadium permeability. Fig. 5 shows *P* of DF-a1 is slightly increased compare to the unmodified membrane DF-a, due to the enlarged hydrophilic pores and decreased thickness caused by the concentrated sulfuric acid sulfonation. So *Selectivity* of DF-a1 is slightly increased. For DF-a2, *Selectivity* of DF-a2 are greatly increased due to the PFSA introduction into the hydrophilic pores as a result of reduction in vanadium permeability (Fig.5).

3.4 Effect of sulfonation on water transfer in VRFB

It is verified that water transfer direction depends on the type of IEM during the VRFB operation [34, 35]. Based on this finding, water transfer can be curbed by introduction cation exchange groups into the anion exchange membrane as a separator in VRFB. Fig. 6 shows that the height deviations of positive and negative vanadium solutions (50% SOC) separated by membrane with time. The water transfer direction is from positive side to the negative side for the unmodified anion exchange membrane DF-a, which is consist to the results by Skyllas-Kazacos. Water transfer across the modified membrane DF-a2 is significantly restrained with a height deviation of 0.1 cm after 120 h, compared to that of 0.65 cm after 120 h for DF-a, which is attributed to the "Donnan" effect [36].

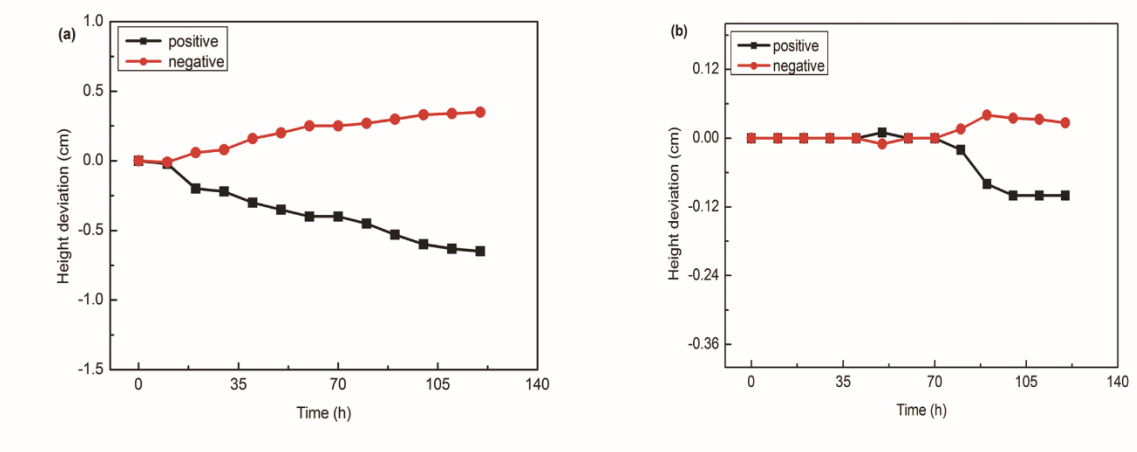

Figure 6. Height evolutions of positive and negative electrolytes (50% SOC) separated by the membrane. (a) DF-a, (b) DF-a2.

3.5 Effect of sulfonation of chemical stability against V(V) solution

Table 5. Chemical stability of membranes after soaking in 1.0 mol/L VO_2^+ solution for 30 d.

membrane	Weight loss(%)	Reduction of VO_2^+(%)
DF-a	22.71	3.0
DF-a1	20.57	2.6
DF-a2	10.34	1.2

The weight losses and percentages of V(V) reduction to V(IV) are list in table 5. After sulfonating, the modified membrane's weight losses the percentages of V(V) reduction are less than

the unmodified membrane. The data of DF-a1 are bigger than DF-a2 indicating the sulfonating type II are more beneficial to improve chemical stability of DF-a membrane.

3.6 OCV

Open circuit voltage (OCV) can be used to indicate the degree of self-discharge of a cell. In this work, OCV of the VRFB was monitored at room temperature after it was charged to a 75% SOC. The OCV of VRFB with DF-a, DF-a1, and DF-a2 membranes are shown in Fig. 7. It can be seen that OCV values with three membranes decreases gradually with the time at first and then drops sharply. The time for OCV value remaining beyond 1.2 V is in the increasing order of DF-a1 (32 h) < DF-a (35 h) < DF-a2 (45 h). The self-discharge of VRB is mainly attributed to the crossover of vanadium ions through the membrane. This result indicates the self-discharge of VRFB has been reduced remarkably by sulfonating type II and the performance of DF-a2 membrane is superior to that of the other two membranes.

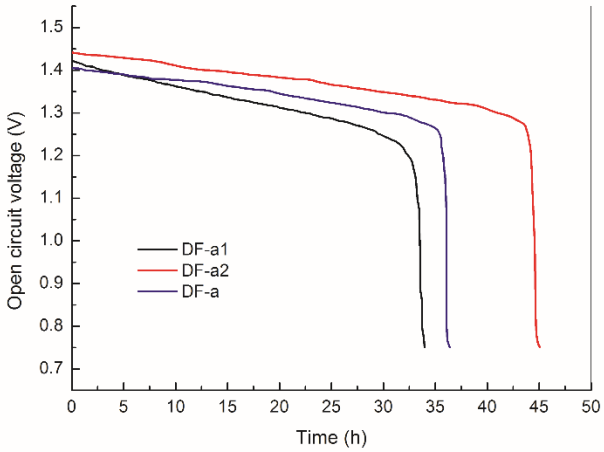

Figure 7. Open circuit voltage (OCV) of VRFB single cell with DF-a, DF-a1, and DF-a2 membranes.

3.7 Cell test

Fig. 8 displays the charge-discharge curves of VRFB single cell employing with DF-a, DF-a1, and DF-a2 membranes at 50 mA/cm^2. The charge voltage of a single cell with DF-a is higher than that with DF-a1 and DF-a2 which is assigned to the lager IR drop caused by the higher AR compared with the other two membranes (Table 4). The charge-discharge capacities with DF-a2 are more than that with DF-a1 and DF-a, which is attribute to the lower self-discharge of the cell with DF-a2 (Fig. 7) and the higher ion selectivity between vanadium ions and H^+ (Table 4).

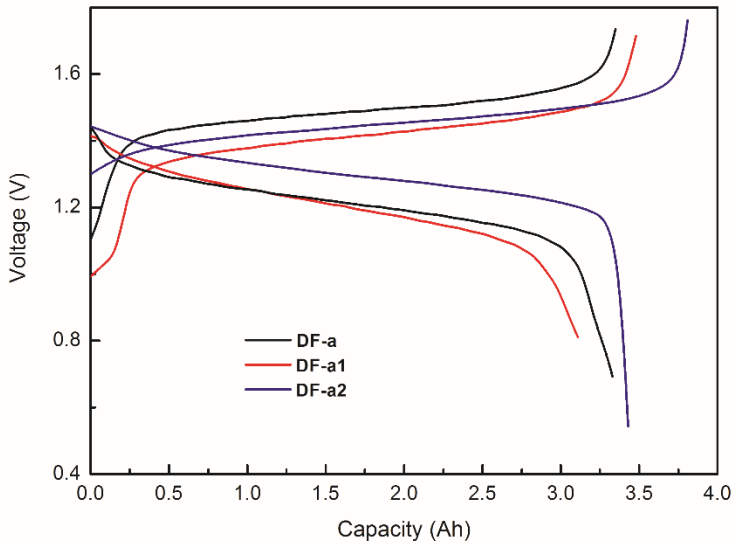

Figure 8. Charge/discharge curves for membranes in VRFB single cell at 50 mA/cm^2.

Table 6 lists the cell performance efficiencies for membranes at 50 mA·cm^{-2} for 80 cycles. The VRFB using DF-a2 presents a *CE* of 98.5%, higher than the values of for DF-a and DF-a1. This is in good agreement with the fact that the high crossover of vanadium ions through the membrane results in a large loss of electrochemical energy [37]. The *VE* of VRFB single cell with DF-a1 is 90.3% higher than that of DF-a and DF-a2, due to the lower area resistance. As an indicator of energy loss in charge-discharge process, *EE* is the key parameter to evaluate an energy storage system. Compared with *EE* value of 80.1% and 80% for DF-a and DF-a1 respectively, the overall *EE* employing DF-a2 membrane was 83.3%, which indicates the DF-a2 has a better potential application in VRFB.

Table 6. The cell performance efficiencies for membranes at 50 mA·cm^{-2}.

Membranes	*CE* (%)	*VE* (%)	*EE* (%)
DF-a	91.8	87.3	80.1
DF-a1	88.6	90.3	80.0
DF-a2	98.5	84.6	83.3

4. CONCLUSIONS

Several conventional ion exchange membrane were studied in terms of their primary properties and an anion exchange membrane DF-a with poly(phenylene oxide) has a potential application in vanadium redox flow battery (VRFB). In order to reduce *WT* in VRFB, DF-a was modified by two sulfonation reactions with concentrated sulfuric acid with potassium dichromate as a catalyst (type I) and with a perfluorinated sulfonic acid solution (type II). The chemical stability of the membrane modified by type II was better than that by type I. After sulfonation, compared to unmodified

membrane DF-a, the modified membranes (DF-a1 and DF-a2) exhibit higher IEC and proton conductivity. Due to Donnan effect, the modified membrane DF-a2 had lower vanadium ions permeability and better ion selectivity and lower self discharge (OCV). DF-a2 had a dramatic reduction in water transfer compared to the unmodified membrane DF-a. VRFB single cell test showed that the DF-a2 had higher energy efficiency than the other two membranes and has a better potential application in VRFB.

ACKNOWLEDGMENTS
We are grateful to Scientific Research Fund of Hunan Provincial Education Department (17K026) and the National Natural Science Foundation of China (81874332） and Hunan Province Key Laboratory of Environmental Catalysis and Waste Recycling (Hunan Institute of Engineering) for the financial support.

References

1. E. Sum, M. Rychcik, M. Skyllas-kazacos, *J. Power Sources*, 16 (1985) 85.
2. E. Sum, M. Skyllas-Kazacos, *J. Power Sources*, 15 (1985) 179.
3. M. Skyllas-Kazacos, F. Grossmith, *J. Electrochem. Soc.*, 134 (1987) 2950.
4. M. Skyllas-Kazacos, M. Rychcik, R.G. Robins, A.G. Fane, M.A. Green, *J. Electrochem. Soc.*, 133 (1986) 1057.
5. T. Mohammadi, M. Skyllas-Kazacos, *J. Membr. Sci.*, 107 (1995) 35.
6. G.J. Hwang, H. Ohya, *J. Membr. Sci.*, 132 (1997) 55.
7. M. Skyllas-Kazacos, D. Kasherman, D.R. Hong, M. Kazacos, *J. Power Sources*, 35 (1991) 399.
8. T. Mohammadi, S.C. Chieng, M. Skyllas Kazacos, *J. Membr. Sci.*, 133 (1997) 151.
9. S. Gu, G. He, X. Wu, C. Li, H. Liu, C. Lin, X. Li, *J. Membr. Sci.*, 281 (2006) 121.
10. S. Kim, J. Yan, B. Schwenzer, J. Zhang, L. Li, J. Liu, Z. Yang, M.A. Hickner, *Electrochem. Commun.*, 12 (2010) 1650.
11. S. Kim, T. Tighe, B. Schwenzer, J. Yan, J. Zhang, J. Liu, Z. Yang, M. Hickner, *J. Appl. Electrochem.*, (2011) 1.
12. Z. Mai, H. Zhang, X. Li, C. Bi, H. Dai, *J. Power Sources*, 196 (2011) 482.
13. D. Chen, S. Wang, M. Xiao, Y. Meng, *J. Power Sources*, 195 (2010) 2089.
14. D. Chen, S. Wang, M. Xiao, Y. Meng, *Energ. Convers. Manage.*, 51 (2010) 2816.
15. D. Chen, S. Wang, M. Xiao, Y. Meng, *Energ. Environ. Sci.*, 3 (2010) 622.
16. X. Chen, P. Chen, Z. An, K. Chen, K. Okamoto, *J. Power Sources*, 196 (2010) 1694.
17. J. Kim, Y. Lee, J.D. Jeon, S.Y. Kwak, *J. Power Sources*, 383 (2018) 1.
18. N. Wang, S. Peng, Y. Li, H. Wang, S. Liu, Y. Liu, *J. Solid State Electrochem.*, 1.
19. K.L. Huang, X.G. Li, S.Q. Liu, N. Tan, L.Q. Chen, *Renew. Energ.*, 33 (2008) 186.
20. B. Tian, C.W. Yan, F.H. Wang, *J. Appl. Electrochem.*, 34 (2004) 1205.
21. X. Li, H. Zhang, Z. Mai, H. Zhang, I. Vankelecom, *Energ. Environ. Sci.*, 4 (2011) 1147.
22. G.J. Hwang, S.W. Kim, D.M. In, D.Y. Lee, C.H. Ryu, *J. Ind. Eng. Chem.*, 60 (2018) 360.
23. G.J. Hwang, H. Ohya, *J. Membr. Sci.*, 140 (1998) 195.
24. T. Sukkar, M. Skyllas-Kazacos, *J. Appl. Electrochem.*, 34 (2004) 137.
25. D. Chen, S. Wang, M. Xiao, D. Han, Y. Meng, *J. Power Sources*, 195 (2010) 7701.
26. G.J. Hwang, H. Ohya, *J. Membr. Sci.*, 120 (1996) 55.
27. S. Sang, Q. Wu, K. Huang, *J. Membr. Sci.*, 305 (2007) 118.
28. N. Wang, S. Peng, H. Wang, Y. Li, S. Liu, Y. Liu, *Electrochem. Commun.*, 17 (2012) 30.
29. J.Y. Xi, Z.H. Wu, X.P. Qiu, L.Q. Chen, *J. Power Sources*, 166 (2007) 531.

30. J. Qiu, J. Zhang, J. Chen, J. Peng, L. Xu, M. Zhai, J. Li, G. Wei, *J. Membr. Sci.*, 334 (2009) 9.
31. D.I. Bower, An Introduction to Polymer Physics, Cambridge University Press, 2002.
32. J.Y. Qiu, L. Zhao, M.L. Zhai, J.F. Ni, H.H. Zhou, J. Peng, J.Q. Li, G.S. Wei, *J. Power Sources*, 177 (2008) 617.
33. K.D. Kreuer, *J. Membr. Sci.*, 185 (2001) 29.
34. T. Mohammadi, M.S. Kazacos, *J. Power Sources*, 63 (1996) 179.
35. T. Sukkar, M. Skyllas-Kazacos, *J. Membr. Sci.*, 222 (2003) 235.
36. T. Mohammadi, M. Skyllas-Kazacos, *J. Membr. Sci.*, 98 (1995) 77.
37. Q.T. Luo, H.M. Zhang, J. Chen, D.J. You, C.X. Sun, Y. Zhang, *J. Membr. Sci.*, 325 (2008) 553.